



# Kahramanmaraş Sutcu Imam University

## Journal of Engineering Sciences



Geliş Tarihi : 27.06.2025  
Kabul Tarihi : 26.07.2025

Received Date : 27.06.2025  
Accepted Date : 26.07.2025

### BIOWASTE TEMPLATED TiO<sub>2</sub> NANOPARTICLES DOPED WITH IRON IONS: STRUCTURAL, MORPHOLOGICAL, AND OPTICAL CHARACTERIZATION

#### DEMİR İYONLARI KATKILI BİYO-ATIK İÇERİKLİ TiO<sub>2</sub> NANO TANECİKLERİ: YAPISAL, MORFOLOJİK VE OPTİKSEL KARAKTERİZASYONU

Nazlı TURKTEN<sup>1</sup> (ORCID: 0000-0001-9343-3697)

Yunus KARATAS<sup>1\*</sup> (ORCID: 0000-0002-3826-463X)

Zekiye CINAR<sup>2</sup> (ORCID: 0009-0008-0377-6126)

<sup>1</sup> Department of Chemistry, Kirsehir Ahi Evran University, 40100, Kirsehir, Türkiye

<sup>2</sup> Department of Chemistry, Yildiz Technical University, 34220, Istanbul, Türkiye

\*Sorumlu Yazar / Corresponding Author: Yunus KARATAS, ykaratas@ahievran.edu.tr

#### ABSTRACT

This study highlighted a facile preparation of a low-cost and efficient iron dopant photocatalyst using rice husk (RH) for water treatment. RH was not only used as a template but also as a multi-dopant source to prepare biowaste-templated TiO<sub>2</sub> nanoparticles with iron ions (RH-Fe-TiO<sub>2</sub>). RH, as an agricultural waste, was used to prepare RH-Fe-TiO<sub>2</sub> nanoparticles through a sol-gel method, followed by iron doping via a wet impregnation method. XRD analysis results indicated that the RH-Fe-TiO<sub>2</sub> specimen contained a mixed phase, primarily composed of anatase and a smaller amount of rutile TiO<sub>2</sub>. The removal of the sacrificial template and the iron doping were confirmed through SEM-EDAX and XPS analysis. FTIR analysis also proved the presence of silicon derived from RH and iron dopant ions resulting from the doping procedure. The morphology of the RH-Fe-TiO<sub>2</sub> specimen exhibited a fibrous and lamellar structure with cracks formed due to the removal of the sacrificial template. The iron doping process resulted in a reduction of the band gap and an observed red shift in the spectrum. The BET surface area of the photocatalyst was found to be 47 m<sup>2</sup>/g. The RH-Fe-TiO<sub>2</sub> catalyst degraded 41% of 4-nitrophenol (4-NP) in 120 min.

**Keywords:** 4-Nitrophenol, biotemplate, biowaste, iron doping, rice husk, photocatalysis.

#### ÖZET

Bu çalışmada, pirinç kabuğu (RH) kullanılması ile düşük maliyetli ve etkili bir demir katkılı fotokatalizörün su arıtımında kullanılması için kolay bir yöntemle sentezi konusu vurgulanmıştır. RH sadece bir şablon olarak kullanılmamış, aynı zamanda çoklu bir katkılandırma kaynağı olarak da demir iyonları içeren biyo-atık içerikli TiO<sub>2</sub> nano taneciklerinin (RH-Fe-TiO<sub>2</sub>) hazırlanmasında kullanılmıştır. RH-Fe-TiO<sub>2</sub> örneğinin hazırlanmasında tarımsal atık olan RH ile sol-jel yöntemi ve ardından ıslak emdirme yöntemi kullanılarak demir katkılandırılması sağlanmıştır. XRD analiz sonuçları, RH-Fe-TiO<sub>2</sub> nano taneciklerinin başlıca anataz fazı ve eser miktarda rutil TiO<sub>2</sub> fazı içeren bir faz karışımından oluştuğunu göstermiştir. SEM-EDAX ve XPS analizleri ile şablonunun uzaklaştırılması ve demir katkısının varlığı doğrulandı. FTIR analizi ile RH'den gelen silikonun ve katkılandırma işleminden oluşan demir iyonlarının varlığı kanıtlanmıştır. RH-Fe-TiO<sub>2</sub> numunesinin morfolojisi, şablonunun uzaklaşması sonucunda oluşan çatlaklar içeren lifli ve lamelli bir yapı göstermiştir. Demir ile katkılandırma işlemi sonucunda, band boşluğu azalmış ve spektrumda kırmızıya doğru bir kayma gözlenmiştir. Fotokatalizörün BET yüzey alanı 47 m<sup>2</sup>/g olarak bulunmuştur. RH-Fe-TiO<sub>2</sub> katalizörü, 4-nitrofenolün (4-NP) %41'ini 120 dakikada giderebilmiştir.

**Anahtar Kelimeler:** 4-Nitrofenol, biyo-şablon, biyo-atık, demir katkılandırma, pirinç kapçığı, fotokataliz.

## INTRODUCTION

Agricultural waste is considered a low-cost, easily accessible, and rich source of lignocellulosic biomass. The improper disposal of enhanced agro-waste can lead to environmental and economic issues, leading to water and soil pollution. Rice husk (RH), sugarcane bagasse, and coconut husk are regarded as sustainable and innovative materials for various applications, including adsorbents or catalysts in water treatment, and as clean alternative fossil fuel energy sources (Liou and Wang, 2025; Sujanto et al., 2024). RH is formed by milling approximately 20% of the total grain weight, primarily comprising silica, cellulose, and mineral components (De Gregori da Rocha et al., 2025). Recently, several studies have been focused on transforming this low-value waste into appreciated products such as biochars, construction materials, polymer composites, supercapacitors, and biosensors in various applications (Onu et al., 2022; Prabha et al., 2021; Suhot et al., 2021).

The increasing trend of manufacturing sectors in industrial countries can cause an environmental threat due to their improper disposal of liquid waste. Common hazardous pollutants in wastewater include pharmaceuticals, dyes, aromatic compounds, phenols, pesticides, and micropollutants, which are frequently released into the environment. Exceeding the permitted levels of these compounds can result in serious consequences (Mohd Zaki et al., 2024). Numerous efforts have been made to eliminate phenol and its substituted compounds from water due to the adverse effects these compounds pose on human health, as they are toxic, carcinogenic, and mutagenic (Bibi et al., 2023; Gurkan et al., 2017; San et al., 2001; San et al., 2002; Sun et al., 2022). Hence, cost-effective and efficient materials for water technologies can help address the issue of water pollution. The utilization of RH highlights the economic concept of “waste to wealth” in this field (Hussain et al., 2024; Yadav and Shrotriya, 2024). Recently, RH biochar and RH biochar-based composites have already been used to remove toxic contaminants from water, regarded as high-value-added either adsorbents or catalysts (Li et al., 2023; Rangarajan et al., 2022; Thuan et al., 2023).

Photocatalysis is a promising and environmentally friendly method for water treatment, which relies on the generation of hydroxyl radicals and superoxide radicals. This phenomenon primarily refers to various semiconductor oxides, such as  $\text{TiO}_2$  and  $\text{ZnO}$ , which play a crucial role in catalytic reactions as photocatalysts. However, these photocatalysts encounter limitations in practical applications due to their large band gap, rapid electron-hole recombination, and lack of visible light activity. Significant strategies have focused on modifying and designing the materials of  $\text{TiO}_2$  to improve its photocatalytic performance (Hong et al., 2022; Mohd Zaki et al., 2024; Zia and Riaz, 2021). In this context, several researchers have utilized RH to prepare efficient RH-derived  $\text{TiO}_2$  photocatalysts (Banu Yener and Helvacı, 2015; Hui et al., 2015; Joseph et al., 2021; Turkten et al., 2023; Wang et al., 2019). Wang et al. prepared mesoporous  $\text{SiO}_2@ \text{TiO}_2$  photocatalysts that effectively eliminate rhodamine B dye under xenon lamp and visible light irradiation (Wang et al., 2019). In another photocatalytic study, rice husk ash was utilized as a  $\text{SiO}_2$  source to prepare  $\text{TiO}_2\text{-SiO}_2$  composites, and their photocatalytic performance was tested on the degradation of terephthalic acid (Banu Yener and Helvacı, 2015). Hui et al. synthesized  $\text{TiO}_2\text{-SiO}_2$  nanoporous composites using RH as a template, reporting a high photocatalytic degradation of methylene blue, achieving up to 82% in 4 hours (Hui et al., 2015).

So far, RH has been employed as a biogenic precursor to develop hierarchical  $\text{TiO}_2$  composites and mesoporous  $\text{TiO}_2$  photocatalysts (de Cordoba et al., 2019; Turkten et al., 2023; Zhaohui et al., 2018). Cordoba et al. synthesized carbon-containing  $\text{TiO}_2\text{-SiO}_2$  photocatalysts using RH as both the silicon source and mesoporous template from the solvothermal treatment (de Cordoba et al., 2019). In another study, RH was employed as a biogenic template to prepare hierarchical MIL-125/ $\text{TiO}_2@ \text{SiO}_2$  composites, and the photocatalytic activity of the composite was evaluated through the degradation of rhodamine B dye (Zhaohui et al., 2018). In our previous study, RH served as both a template and a source of dopants to synthesize a hierarchical microstructure  $\text{TiO}_2$  photocatalyst via the sol-gel method, which incorporated multiple dopant elements resulting from the calcination of RH (Turkten et al., 2023). This hierarchical microstructure of  $\text{TiO}_2$  exhibited a higher photocatalytic activity on the degradation of 4-nitrophenol (4-NP) compared to  $\text{TiO}_2$  nanoparticles.

Iron doping with  $\text{TiO}_2$  has emerged as one of the most effective options among transition metal ions due to its cation radius being nearly identical to that of  $\text{Ti}^{4+}$ . This offers a strategy for enhancing the visible light region response of  $\text{TiO}_2$  (Jahantiq et al., 2020; Matias et al., 2022). In our previous studies, the various methods for preparing iron-doped  $\text{TiO}_2$  and their effects on humic acid degradation and characterization were investigated (Birben et al., 2017; Türkten and Uyguner Demirel, 2020). Yalcin et al. Fe-doped  $\text{TiO}_2$  photocatalysts were synthesized using commercial P25 via

a wet impregnation method, indicating a high photocatalytic degradation of 4-NP. They reported that the presence of the additional electronic states could result in visible light activity of the photocatalyst (Yalçın et al., 2010). Herein, a value-added photocatalyst used in water treatment, originating from an agricultural waste, RH, was proposed. Therefore, RH was proposed as an economical, self-sacrificing bio-template and a derived multi-dopant source for preparing TiO<sub>2</sub> nanoparticles with iron ions. FTIR, XRD, SEM, BET, XPS, and UV-DRS spectroscopy tools were employed to analyze the structural, morphological, optical, and surface characteristic properties of the photocatalyst. 4-NP was chosen as a recalcitrant organic pollutant to evaluate the photocatalytic activity of RH-templated TiO<sub>2</sub> nanoparticles with iron ions (RH-Fe-TiO<sub>2</sub>) under visible light irradiation.

## MATERIALS AND METHODS

Titanium(IV) isopropoxide (TIP) was obtained from Aldrich. Ethanol, 4-nitrophenol (4-NP), hydrochloric acid (HCl), and iron(III) nitrate (Fe(NO<sub>3</sub>)<sub>3</sub>·9H<sub>2</sub>O) were purchased from Merck and used without further purification in the analyses. RH-templated TiO<sub>2</sub> nanoparticles were synthesized using a sol-gel method, as detailed in our previous study (Turkten et al., 2023). Iron doping (0.5wt% Fe) was prepared by an incipient wet impregnation method as reported in our previous research (Birben et al., 2017). Briefly, 10 g of RH-templated TiO<sub>2</sub> nanoparticles containing 0.36 g Fe(NO<sub>3</sub>)<sub>3</sub>·9H<sub>2</sub>O in 10 mL distilled water were stirred on a magnetic stirrer for 1 h. Then, RH-Fe-TiO<sub>2</sub> particles were washed, dried, calcined at 500°C for 5 h, ground, and sieved. Comprehensive details on the characterization analysis were discussed in our previous study (Turkten et al., 2023). Crystallite size (D, nm) of RH-Fe-TiO<sub>2</sub> nanoparticles was calculated using the Scherrer equation (Scherrer, 1918). The band-gap energy of the RH-Fe-TiO<sub>2</sub> specimen was calculated using the Kubelka-Munk equation (Kubelka and Munk, 1931). From plotting the Tauc formula of [F(R).hv]<sup>n</sup> vs hv (photon energy, eV and n=1/2), the band-gap energy was deduced by the linear intersection of this plot's extrapolation. The photocatalytic activity of RH-Fe-TiO<sub>2</sub> nanoparticles (0.2 g/100 mL) was evaluated on the degradation of 4-NP (1x10<sup>-4</sup> mol/L) in a 600 mL suspension, which was placed in a double-jacket Pyrex photoreactor. The photocatalytic tests were conducted without adjusting the pH, which remained approximately at pH=6 throughout the experiments. Detailed information on photocatalytic experiments was also reported in our previous study (Turkten et al., 2023).

## RESULTS AND DISCUSSION

### Characterization of RH-Fe-TiO<sub>2</sub> Nanoparticles

The characteristic properties of RH and TiO<sub>2</sub> nanoparticles were identified in our previous study (Turkten et al., 2023). XRD diffractogram of RH-Fe-TiO<sub>2</sub> nanoparticles revealed the diffraction peaks at 2θ=25.16, 37.38°, 38.42°, 47.84°, 53.66°, 54.60°, and 62.37° related to the (1 0 1), (0 0 4), (1 1 2), (2 0 0), (1 0 5), (2 1 1), and (0 0 2) reflection planes of anatase TiO<sub>2</sub>, respectively (JCPDS No. 73–1764), and a minor rutile peak at 2θ=27.33° corresponded to (1 1 0) plane (JCPDS No. 99–0090) (Figure 1 (a)). No characteristic crystalline phases corresponding to iron, such as Fe<sub>2</sub>TiO<sub>5</sub> and α-Fe<sub>2</sub>O<sub>3</sub>, were detected. The reason could be a low calcination doping process, preventing Fe<sup>3+</sup> cations from reacting with TiO<sub>2</sub> and forming these crystalline phases (Yalçın et al., 2010). The crystallite particle size of RH-

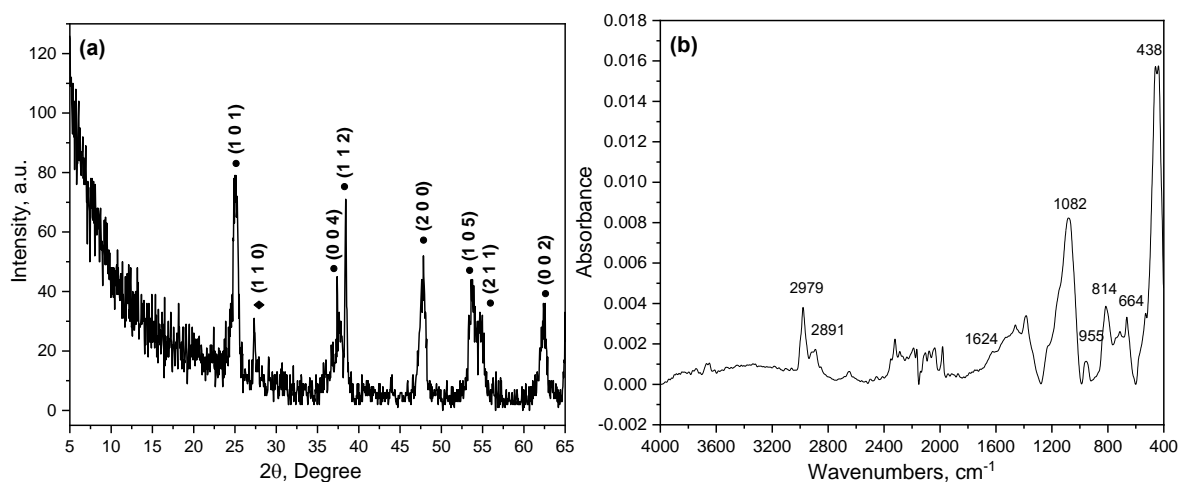


**Figure 1.** (a) XRD Diffractogram (•Anatase and◆Rutile) and (b) FTIR Spectrum of RH-Fe-TiO<sub>2</sub> Specimen.

Fe-TiO<sub>2</sub> nanoparticles was 13.8 nm. Yelda et al. reported a slightly higher crystallite particle size value (17.9 nm) for the 0.50 wt% Fe<sup>3+</sup>-TiO<sub>2</sub> photocatalyst, which was prepared by a wet impregnation method (Yalçın et al., 2010).

FTIR spectrum of RH-Fe-TiO<sub>2</sub> nanoparticles revealed peaks at 2971 cm<sup>-1</sup> and 2891 cm<sup>-1</sup>, which were assigned to the stretching of C-H and originated from -CH<sub>2</sub> and -CH<sub>3</sub> of TTIP (Kapridaki et al., 2019) (Figure (b)). The peak at 1624 cm<sup>-1</sup> belonged to the bending vibration of adsorbed water. In the spectral region, the absorption peaks below around 950 cm<sup>-1</sup> were related to the Ti-O stretching and O-Ti-O bending vibrations. The observed three additional peaks at 1082 cm<sup>-1</sup>, 814 cm<sup>-1</sup>, and 438 cm<sup>-1</sup> could be attributed to RH, indicating that TiO<sub>2</sub> was coated onto the biogenic template. The peak at 1082 cm<sup>-1</sup> corresponded to the C-OH and Si-O vibrations in siloxane, whereas the peaks at 814 cm<sup>-1</sup> and 438 cm<sup>-1</sup> related to the symmetric Si-O and Si-O-Si bending vibrations, respectively (Turkten et al., 2023). The observed peak at 664 cm<sup>-1</sup> could be attributed to the Fe-O stretching vibration (Jayasaranya et al., 2024).

SEM images and EDAX spectra of RH and RH-Fe-TiO<sub>2</sub> nanoparticles are presented in Figure 2. The morphology of the RH featured a fibrous structure that was both longitudinal and lamellar. In contrast, the RH-Fe-TiO<sub>2</sub> specimen

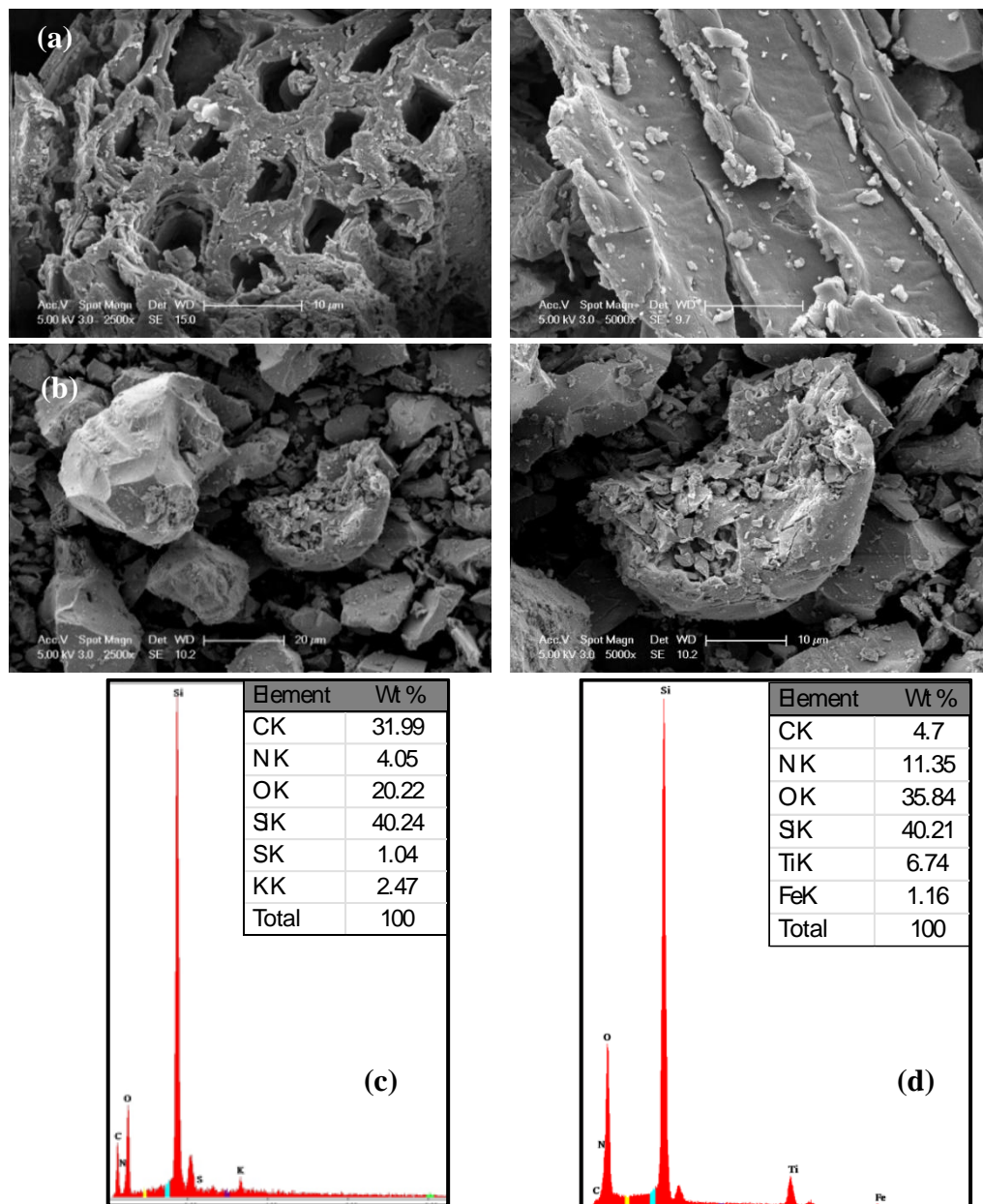


**Figure 2.** SEM Images of x2500 (left) and x5000 (right), (a) RH and (b) RH-Fe-TiO<sub>2</sub>, and EDAX Spectra of RH- (c) RH and (d) RH- Fe-TiO<sub>2</sub> Specimens.

revealed a hierarchical matrix within the cracks formed by the burned biogenic template. The dominant elements were Si, C, and O atoms in both EDAX spectra. The detection of derived elements from RH and iron in the EDAX spectra of RH-Fe-TiO<sub>2</sub> confirmed the calcination of the biogenic template and indicated a successful doping process.

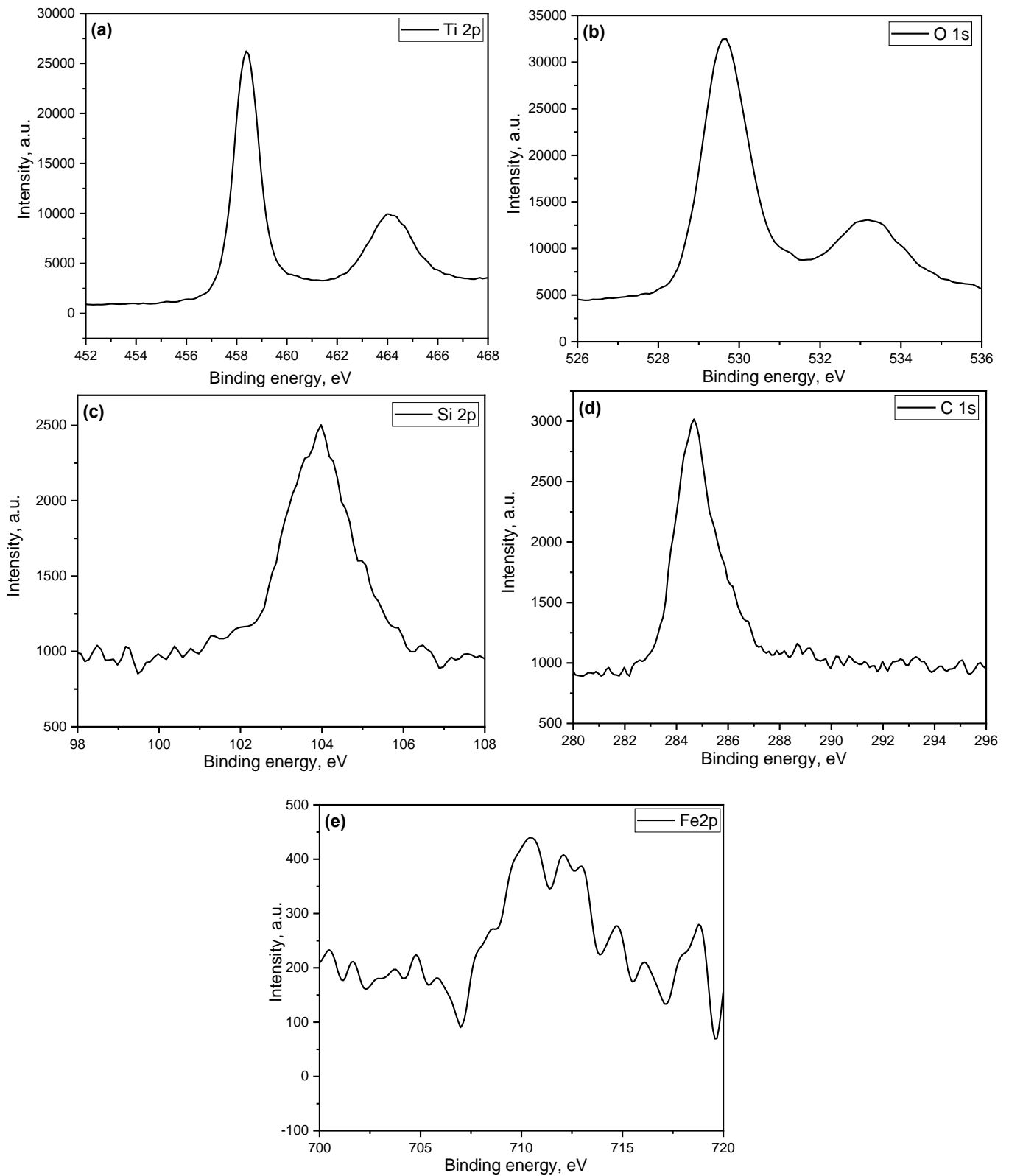


**Figure 3.** XPS Spectra of (a) Ti 2p, (b) O 1s, (c) Si 2p, (d) C 1s, and (e) Fe 2p Core Level of RH-Fe-TiO<sub>2</sub> Nanoparticles.

XPS spectra of RH-Fe-TiO<sub>2</sub> nanoparticles consisted of five spectral regions corresponding to Ti 2p, O 1s, Si 2p, C 1s, and Fe 2p (Figure 3). In the Ti 2p XPS spectrum, the peaks at 458.1 eV and 464.2 eV were attributed to the Ti 2p<sub>1/2</sub> and Ti 2p<sub>3/2</sub> states of TiO<sub>2</sub>, respectively, indicating a Ti<sup>4+</sup> oxidation state. For the O 1s energy core level, two binding energies were observed at 529.7 eV and 533.2 eV, corresponding to the metallic oxides and Si–O bond derived from the calcined biogenic template, respectively. The Si 2p core level exhibited a binding energy peak at 103.9 eV, belonging to the Si 2p<sub>1/2</sub>. Considering the C 1s core level, a major peak at 284.7 eV was assigned to the C sp<sup>2</sup> graphitic carbon (Turkten et al., 2023). In the Fe 2p core level spectrum, a characteristic peak was detected at 710.5 eV, corresponding to Fe 2p<sub>3/2</sub>, which revealed that the oxidation state of Fe was (III) (Hung et al., 2008). The XPS results were confirmed by both the SEM analysis and the EDAX. This also indicated that multi-doped elements were derived from the calcination of the biogenic template and successful iron doping.

Nitrogen adsorption-desorption plot of RH-Fe-TiO<sub>2</sub> nanoparticles (Figure 4 (a)) revealed a Type IV isotherm according to IUPAC classification (Sing, 1985). BET surface area of RH-Fe-TiO<sub>2</sub> nanoparticles was 47 m<sup>2</sup>/g. The UV-DRS spectrum of RH-Fe-TiO<sub>2</sub> nanoparticles revealed a distinct absorption edge at approximately 340 nm, extending to around 480 nm, and then to 690 nm (Figure 4 (b)). The band gap energy of the RH-Fe-TiO<sub>2</sub> specimen was 2.62 eV (λ = 474 nm). In our previous study, the band gap of TiO<sub>2</sub> hierarchical microstructure was found to be 2.74 eV (λ = 452 nm). The iron doping process could result in additional doping energy levels, leading to a decrease in the band gap and a red shift (Turkten et al., 2023). The introduction of additional doping energy levels within the band gap was responsible for this change (Yalçın et al., 2010).

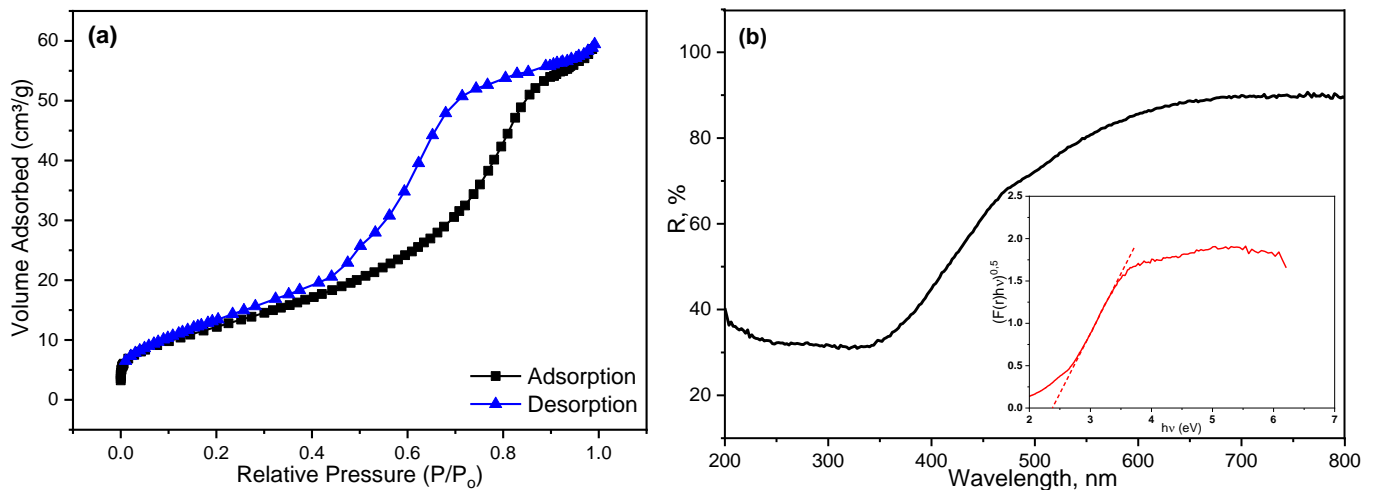


**Figure 4.** RH-Fe-TiO<sub>2</sub> Nanoparticles (a) N<sub>2</sub> Adsorption-Desorption (b) UV-DRS Spectra.

### Photocatalytic Activity of RH-Fe-TiO<sub>2</sub> nanoparticles

The photocatalytic activity of RH-Fe-TiO<sub>2</sub> nanoparticles on the degradation of 4-NP was investigated in 120 minutes of UV light irradiation (Figure 5).

The percent removal of 4-NP was calculated using Equation (1).

$$\text{Degradation, \%} = \left( \frac{C_o - C_t}{C_o} \right) \times 100 \quad (1)$$

where,

$C_o$  : initial concentration of 4-NP,

$C_t$  : concentration of 4-NP at time  $t$ .

The removal efficiency of 4-NP in the presence of the RH-Fe-TiO<sub>2</sub> specimen was 41% after 120 min. It was reported that the iron doping process of TiO<sub>2</sub> resulted in reduced electron/hole recombination and improved charge separation, because Fe<sup>3+</sup> dopant ions could serve as recombination centers (Komaraiah et al., 2019). Yelda et al. reported that

the iron doping amount affected the photocatalytic activity, and they found the photocatalytic degradation of 4-NP varied between 64% and 80% (Yalçın et al., 2010).

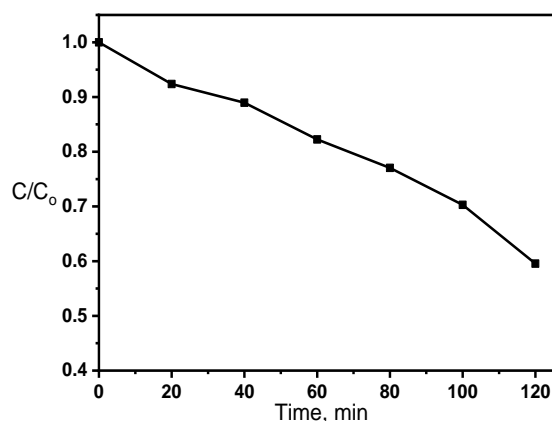


Figure 5. Removal Efficiencies of RH-Fe-TiO<sub>2</sub> Nanoparticles.

## CONCLUSION

In this current study, RH-Fe-TiO<sub>2</sub> nanoparticles were synthesized from a biowaste, RH, using a sol-gel method, followed by iron doping through a wet impregnation process. RH was applied as both a sacrificial template and a multi-dopant source, such as Si, C, and N. The removal of RH in the photocatalyst after a calcination process resulted in a similar sacrificial template morphology that formed in the cracks of a fibrous structure. The crystallite particle size of RH-Fe-TiO<sub>2</sub> nanoparticles was 13.8 nm, and both anatase and a minor rutile phase of TiO<sub>2</sub> were detected. XPS results confirmed the sacrificial template and iron doping process. The BET surface area of the RH-Fe-TiO<sub>2</sub> specimen was 47 m<sup>2</sup>/g and revealed a Type IV isotherm. According to UV-DRS analysis, the band gap energy of the RH-Fe-TiO<sub>2</sub> specimen was 2.62 eV, and the iron doping procedure resulted in a red shift. Through photocatalytic results, it was found that the removal efficiency of 4-NP was 41% in 120 min. The results of this study emphasized that agricultural biowaste can be transformed into a valuable photocatalyst for water treatment.

The present article is dedicated to the memory of Prof. Dr. Zekiye Cinar, who passed away on July 22, 2021.

## Artificial Intelligence Contribution Statement

This manuscript was entirely written, edited, analyzed, and prepared without the assistance of any artificial intelligence tools. All content, including text, data analysis, and figures, was solely generated by the authors.

## REFERENCES

- Banu Yener, H., & Helvacı, Ş. Ş. (2015). Effect of synthesis temperature on the structural properties and photocatalytic activity of TiO<sub>2</sub>/SiO<sub>2</sub> composites synthesized using rice husk ash as a SiO<sub>2</sub> source. *Separation and Purification Technology*, 140, 84-93. <https://doi.org/https://doi.org/10.1016/j.seppur.2014.11.013>
- Bibi, A., Bibi, S., Abu-Dieyeh, M., & Al-Ghouti, M. A. (2023). Towards sustainable physiochemical and biological techniques for the remediation of phenol from wastewater: A review on current applications and removal mechanisms. *Journal of Cleaner Production*, 417, 137810. <https://doi.org/https://doi.org/10.1016/j.jclepro.2023.137810>
- Birben, N. C., Uyguner-Demirel, C. S., Kavurmaci, S. S., Gürkan, Y. Y., Turkten, N., Cinar, Z., & Bekbolet, M. (2017). Application of Fe-doped TiO<sub>2</sub> specimens for the solar photocatalytic degradation of humic acid. *Catalysis Today*, 281, 78-84. <https://doi.org/10.1016/j.cattod.2016.06.020>
- de Cordoba, M. C. F., Matos, J., Montaña, R., Poon, P. S., Lanfredi, S., Praxedes, F. R., Hernández-Garrido, J. C., Calvino, J. J., Rodríguez-Aguado, E., Rodríguez-Castellón, E., & Ania, C. O. (2019). Sunlight photoactivity of rice husks-derived biogenic silica. *Catalysis Today*, 328, 125-135. <https://doi.org/https://doi.org/10.1016/j.cattod.2018.12.008>

- De Gregori da Rocha, J., Santana Junior, M. B., Pier Macuvele, D. L., Riella, H. G., Ienczak, J. L., Padoin, N., & Soares, C. (2025). Uncovering engineering and mechanistic insights in green synthesis of carbon dots from rice husks. *Chemical Engineering Journal*, 505, 159364. <https://doi.org/https://doi.org/10.1016/j.cej.2025.159364>
- Gurkan, Y., Kasapbasi, E., Turkten, N., & Cinar, Z. (2017). Influence of Se/N Codoping on the Structural, Optical, Electronic and Photocatalytic Properties of TiO<sub>2</sub>. *Molecules*, 22(3), 414. <http://www.mdpi.com/1420-3049/22/3/414>
- Hong, J., Cho, K.-H., Presser, V., & Su, X. (2022). Recent advances in wastewater treatment using semiconductor photocatalysts. *Current Opinion in Green and Sustainable Chemistry*, 36, 100644. <https://doi.org/https://doi.org/10.1016/j.cogsc.2022.100644>
- Hui, C., Lei, Z., Xitang, W., Shujing, L., & Zhongxing, L. (2015). Preparation of Nanoporous TiO<sub>2</sub>/SiO<sub>2</sub> Composite with Rice Husk as Template and Its Photocatalytic Property. *Rare Metal Materials and Engineering*, 44(7), 1607-1611. [https://doi.org/https://doi.org/10.1016/S1875-5372\(15\)30101-6](https://doi.org/https://doi.org/10.1016/S1875-5372(15)30101-6)
- Hung, W.-C., Chen, Y.-C., Chu, H., & Tseng, T.-K. (2008). Synthesis and characterization of TiO<sub>2</sub> and Fe/TiO<sub>2</sub> nanoparticles and their performance for photocatalytic degradation of 1,2-dichloroethane. *Applied Surface Science*, 255(5, Part 1), 2205-2213. <https://doi.org/https://doi.org/10.1016/j.apsusc.2008.07.079>
- Hussain, M., Aadil, M., Cochran, E. W., Zulfiqar, S., Hassan, W., Kousar, T., Somaily, H. H., & Mahmood, F. (2024). Facile synthesis of a porous sorbent derived from the rice husk biomass: A new and highly efficient material for water remediation. *Inorganic Chemistry Communications*, 160, 112010. <https://doi.org/https://doi.org/10.1016/j.inoche.2023.112010>
- Jahantiq, A., Ghanbari, R., Panahi, A. H., Ashrafi, S. D., Khatibi, A. D., Noorabadi, E., Meshkinian, A., & Kamani, H. (2020). Photocatalytic degradation of 2,4,6-trichlorophenol in aqueous solutions using synthesized Fe-doped TiO<sub>2</sub> nanoparticles via response surface methodology. *Desalination and Water Treatment*, 183, 366-373. <https://doi.org/https://doi.org/10.5004/dwt.2020.25249>
- Jayasaranya, N., Pavai, R. E., Sagadevan, S., Balu, L., & Manoharan, C. (2024). Enhanced room temperature gas sensing performance of iron-doped titanium dioxide nanocomposite. *Applied Physics A*, 130(8), 539. <https://doi.org/10.1007/s00339-024-07688-0>
- Joseph, C. G., Taufiq-Yap, Y. H., Musta, B., Sarjadi, M. S., & Elilarasi, L. (2021). Application of Plasmonic Metal Nanoparticles in TiO<sub>2</sub>-SiO<sub>2</sub> Composite as an Efficient Solar-Activated Photocatalyst: A Review Paper [Review]. *Frontiers in Chemistry*, Volume 8 - 2020. <https://doi.org/10.3389/fchem.2020.568063>
- Kapridaki, C., Xynidis, N., Vazgiouraki, E., Kallithrakas-Kontos, N., & Maravelaki-Kalaitzaki, P. (2019). Characterization of Photoactive Fe-TiO<sub>2</sub> Lime Coatings for Building Protection: The Role of Iron Content. *Materials*, 12(11), 1847. <https://www.mdpi.com/1996-1944/12/11/1847>
- Komaraiah, D., Radha, E., Kalarikkal, N., Sivakumar, J., Ramana Reddy, M. V., & Sayanna, R. (2019). Structural, optical and photoluminescence studies of sol-gel synthesized pure and iron doped TiO<sub>2</sub> photocatalysts. *Ceramics International*, 45(18, Part B), 25060-25068. <https://doi.org/https://doi.org/10.1016/j.ceramint.2019.03.170>
- Kubelka, P., & Munk, F. A. (1931). Contribution to the optics of pigments. *Zeitschrift für technische Physik*, 12, 593-599.
- Li, Z., Zheng, Z., Li, H., Xu, D., Li, X., Xiang, L., & Tu, S. (2023). Review on Rice Husk Biochar as an Adsorbent for Soil and Water Remediation. *Plants*, 12(7), 1524. <https://www.mdpi.com/2223-7747/12/7/1524>
- Liou, T.-H., & Wang, S.-Y. (2025). Utilizing rice husk for sustainable production of mesoporous titania nanocomposites with highly adsorption and photocatalysis. *Biomass and Bioenergy*, 199, 107950. <https://doi.org/https://doi.org/10.1016/j.biombioe.2025.107950>
- Matias, M. L., Pimentel, A., Reis-Machado, A. S., Rodrigues, J., Deuermeier, J., Fortunato, E., Martins, R., & Nunes, D. (2022). Enhanced Fe-TiO<sub>2</sub> Solar Photocatalysts on Porous Platforms for Water Purification. *Nanomaterials*, 12(6), 1005. <https://www.mdpi.com/2079-4991/12/6/1005>

- Mohd Zaki, R. S. R., Jusoh, R., Chanakaewsomboon, I., & Setiabudi, H. D. (2024). Recent advances in metal oxide photocatalysts for photocatalytic degradation of organic pollutants: A review on photocatalysts modification strategies. *Materials Today: Proceedings*, 107, 59-67. <https://doi.org/https://doi.org/10.1016/j.matpr.2023.07.102>
- Onu, C. E., Ohale, P. E., Obiora-Okafo, I. A., Asadu, C. O., Okoye, C. C., Ojukwu, E. V., & Ezennajiego, E. E. (2022). Application of Rice Husk-Based Biomaterial in Textile Wastewater Treatment. In S. S. Muthu & A. Khadir (Eds.), *Textile Wastewater Treatment: Sustainable Bio-nano Materials and Macromolecules, Volume 2* (pp. 231-250). Springer Nature Singapore. [https://doi.org/10.1007/978-981-19-2852-9\\_12](https://doi.org/10.1007/978-981-19-2852-9_12)
- Prabha, S., Durgalakshmi, D., Rajendran, S., & Lichtfouse, E. (2021). Plant-derived silica nanoparticles and composites for biosensors, bioimaging, drug delivery and supercapacitors: a review. *Environmental Chemistry Letters*, 19(2), 1667-1691. <https://doi.org/10.1007/s10311-020-01123-5>
- Rangarajan, G., Jayaseelan, A., & Farnood, R. (2022). Photocatalytic reactive oxygen species generation and their mechanisms of action in pollutant removal with biochar supported photocatalysts: A review. *Journal of Cleaner Production*, 346, 131155. <https://doi.org/https://doi.org/10.1016/j.jclepro.2022.131155>
- San, N., Hatipoğlu, A., Koçtürk, G., & Çınar, Z. (2001). Prediction of primary intermediates and the photodegradation kinetics of 3-aminophenol in aqueous TiO<sub>2</sub> suspensions. *Journal of Photochemistry and Photobiology A: Chemistry*, 139(2-3), 225-232. [https://doi.org/http://dx.doi.org/10.1016/S1010-6030\(01\)00368-9](https://doi.org/http://dx.doi.org/10.1016/S1010-6030(01)00368-9)
- San, N., Hatipoğlu, A., Koçtürk, G., & Çınar, Z. (2002). Photocatalytic degradation of 4-nitrophenol in aqueous TiO<sub>2</sub> suspensions: Theoretical prediction of the intermediates. *Journal of Photochemistry and Photobiology A: Chemistry*, 146(3), 189-197. [https://doi.org/http://dx.doi.org/10.1016/S1010-6030\(01\)00620-7](https://doi.org/http://dx.doi.org/10.1016/S1010-6030(01)00620-7)
- Scherrer, P. (1918). Estimation of the size and internal structure of colloidal particles by means of röntgen. *Nachrichten von der Gesellschaft der Wissenschaften zu Göttingen*, 2, 96-100.
- Sing, K. S. W. (1985). Reporting physisorption data for gas/solid systems with special reference to the determination of surface area and porosity (Recommendations 1984). In *Pure and Applied Chemistry* (Vol. 57, pp. 603).
- Suhot, M. A., Hassan, M. Z., Aziz, S. a. A., & Md Daud, M. Y. (2021). Recent Progress of Rice Husk Reinforced Polymer Composites: A Review. *Polymers*, 13(15), 2391. <https://www.mdpi.com/2073-4360/13/15/2391>
- Sujanto, R. Y., Herrera, S. G. M., & Negash, Y. T. (2024). Enhancing environmental sustainability in a Circular Waste Bioeconomy: A hierarchical framework driven by operational efficiency and agro-energy management. *Cleaner and Circular Bioeconomy*, 9, 100115. <https://doi.org/https://doi.org/10.1016/j.clcb.2024.100115>
- Sun, J., Mu, Q., Kimura, H., Murugadoss, V., He, M., Du, W., & Hou, C. (2022). Oxidative degradation of phenols and substituted phenols in the water and atmosphere: a review. *Advanced Composites and Hybrid Materials*, 5(2), 627-640. <https://doi.org/10.1007/s42114-022-00435-0>
- Thuan, D. V., Chu, T. T. H., Thanh, H. D. T., Le, M. V., Ngo, H. L., Le, C. L., & Thi, H. P. (2023). Adsorption and photodegradation of micropollutant in wastewater by photocatalyst TiO<sub>2</sub>/rice husk biochar. *Environmental Research*, 236, 116789. <https://doi.org/https://doi.org/10.1016/j.envres.2023.116789>
- Turkten, N., Karatas, B., Karatas, Y., Cinar, Z., & Bekbolet, M. (2023). A facile synthesis of bio-inspired hierarchical microstructure TiO<sub>2</sub>: Characterization and photocatalytic activity. *Environmental Progress & Sustainable Energy*, 42(3), e14054. <https://doi.org/https://doi.org/10.1002/ep.14054>
- Türkten, N., & Uyguner Demirel, C. S. (2020). Photocatalytic Activity of in-situ Fe-Doped TiO<sub>2</sub> for Natural Organic Matter Removal [Organik madde giderimi için eş anli (in-situ) fe-katkili tlo<sub>2</sub>'nin fookatalitik aktivitesi]. *Mühendislik Bilimleri ve Tasarım Dergisi*, 8(3), 664-670. <https://doi.org/10.21923/jesd.672750>
- Wang, W., Chen, H., Fang, J., & Lai, M. (2019). Large-scale preparation of rice-husk-derived mesoporous SiO<sub>2</sub>@TiO<sub>2</sub> as efficient and promising photocatalysts for organic contaminants degradation. *Applied Surface Science*, 467-468, 1187-1194. <https://doi.org/https://doi.org/10.1016/j.apsusc.2018.10.275>
- Yadav, V., & Shrotriya, S. (2024). *Waste-to-Wealth*. <https://doi.org/10.1201/9781003327646>

Yalçın, Y., Kılıç, M., & Çınar, Z. (2010). Fe<sup>+3</sup>-doped TiO<sub>2</sub>: A combined experimental and computational approach to the evaluation of visible light activity. *Applied Catalysis B: Environmental*, 99(3-4), 469-477. <https://doi.org/10.1016/j.apcatb.2010.05.013>

Zhaohui, H., Hui, C., Lei, Z., Xuan, H., Weixin, L., Wei, F., & Guanghui, W. (2018). Biogenic Hierarchical MIL-125/TiO<sub>2</sub>@SiO<sub>2</sub> Derived from Rice Husk and Enhanced Photocatalytic Properties for Dye Degradation. *Photochemistry and Photobiology*, 94(3), 512-520. <https://doi.org/https://doi.org/10.1111/php.12873>

Zia, J., & Riaz, U. (2021). Photocatalytic degradation of water pollutants using conducting polymer-based nanohybrids: A review on recent trends and future prospects. *Journal of Molecular Liquids*, 340, 117162. <https://doi.org/https://doi.org/10.1016/j.molliq.2021.117162>